Nonlinear Phenomena in Complex Systems, vol. **25**, no. 4 (2022), pp. 341 - 348

Numerical Simulation of Photoacoustic Effect in One-Dimensional Carbon Nanostructures

Oleg Romanov* and Igor Timoshchenko†
Faculty of Physics, Belarusian State University,
4 Nezalezhnasti Ave., 220030 Minsk, BELARUS
(Received 01 October, 2022)

The paper describes methods for theoretical and numerical simulation of the photoacoustic effect that occurs in one-dimensional carbon micro- and nanostructures under an action of pulsed laser radiation. The proposed numerical modeling technique is based on solving the equations of motion of continuous media in the Lagrange form for spatially inhomogeneous media. This model makes it possible to calculate fields of temperature, pressure, density, and velocity of the medium depending on the parameters of laser pulses and characteristics of micro- and nanostructures.

PACS numbers: 78.20.Hp, 43.35.Sx, 61.46+w
Keywords: photoacoustic effect, laser pulses, carbon nanostructures, numerical simulations
DOI: https://doi.org/10.33581/1561-4085-2022-25-4-341-348

1. Introduction

The photoacoustic effect is the excitation of acoustic pulses in the environment due to rapid heating and expansion of an absorbing particles or structure upon absorption of electromagnetic radiation. At present, the photoacoustic effect is widely used in biomedical research [1], photoacoustic spectroscopy [2], and other applications. Of particular interest is the study of the interaction of pulsed laser radiation with absorbing micro- and nanostructures, since the frequency of excited acoustic oscillations in such structures can reach values from giga- to terahertz. Such oscillations are of particular interest for fundamental research and have many potential applications (acoustic visualization of nanoobjects, acoustic nanocavities, phononic crystals) [3–7].

This work is devoted to the development of a technique for modeling the problems of thermooptical excitation of acoustic vibrations in absorbing one-dimensional carbon micro- and nanostructures. The simulation technique is based on the numerical solution of the equations of motion of continuous media in the Lagrange form. Using the developed technique, the problems of excitation of ultrahigh-frequency oscillations in planar, cylindrical and spherical carbon micro-, nanostructures are considered.

2. Theoretical model

We assume that the liquid medium (water) contains inclusions in the form of carbon particles or structures of various geometry and sufficiently low concentration [8], which differ from the environment in their physical parameters (absorption coefficient, density, etc.). The processes of generation and propagation of acoustic disturbances in such a system will be considered at the level of a single inclusion, that is, for a single carbon particle or structure.

The processes occurring in a continuous medium under the action of pulsed laser radiation can be described by the equations of motion of the medium in the form of Euler or Lagrange [9]. In this work, we use the Lagrange form, since this approach allows us to describe the motion of inhomogeneous (multilayer) media and structures whose properties change when passing through

*E-mail: romanov@bsu.by
†E-mail: TimoshchenkoIA@bsu.by

interfaces.

Next, we consider the problems of absorption of laser radiation in a flat layer (flat geometry, Fig. 1a), as well as in cylindrically and spherically symmetric structures (Fig. 1b, c), which, by their physical characteristics differ from the environment (a cylindrically symmetrical object absorbing radiation or a spherical particle immersed in a medium with different properties).

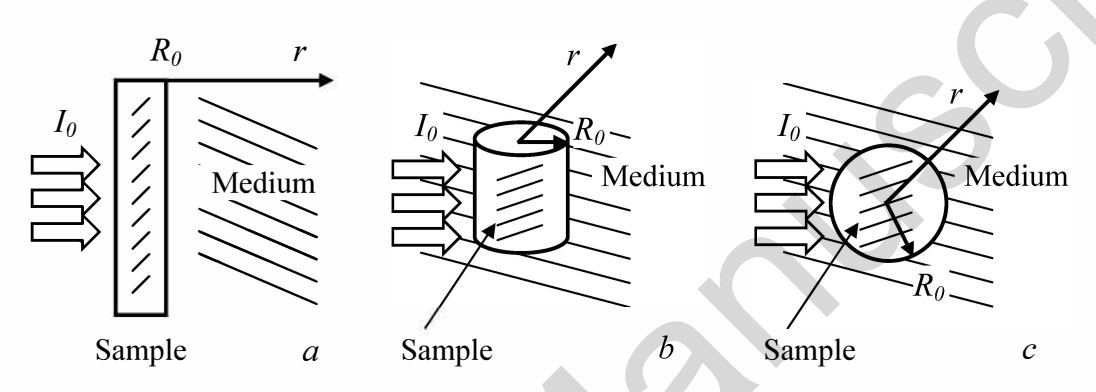

FIG. 1: Scheme of interaction in (a) plane, (b) cylindrical, and (c) spherical geometries.

The system of equations of motion of a continuous medium consists of the equation of continuity, the equations of motion, the equation of energy balance and the equation of state. In the Lagrangian formulation for one-dimensional motion along coordinate r, these equations have the form [10]:

- a continuity equation:

$$V = V_0 \left(\frac{R}{r}\right)^{\alpha-1} \frac{\partial R}{\partial r}; \qquad (1)$$

- equation of motion:

$$\frac{\partial u}{\partial t} = -V_0 \left(\frac{R}{r}\right)^{\alpha-1} \frac{\partial P}{\partial r}; \qquad (2)$$

- equation for changing Euler coordinate R:

$$\frac{\partial R}{\partial t} = u; \qquad (3)$$

- an equation of state:

$$P = P\left(V,\ E\right). \qquad (4)$$

Here, P is the pressure; $V_0 = 1/\rho_0$, $V = 1/\rho$ are the initial and current specific volumes; ρ_0, ρ are the corresponding densities; E is the specific internal energy, r is the Lagrangian coordinate, t is the time, $\alpha = 1, 2, 3$ respectively for the plane, cylindrical and spherical geometry of the problem.

As the equation of states of an absorbing medium and surrounding medium, the Mie-Grüneisen equation in its two-term form (cold, and hot parts) has been used [11]:

$$P = \rho_0 u_0^2 \left(1 - \frac{V}{V_0}\right) + \Gamma \frac{C_V\left(T - T_0\right)}{V}. \qquad (5)$$

Here, $\Gamma = \frac{u_0^2 \beta}{C_V}$ is the Grüneisen coefficient of the medium, C_V is the heat capacity, β is the volume expansion coefficient, u_0 is the sound speed in the medium.

To describe the heating of the medium upon absorption of the laser radiation energy, the following heat conduction equation has been used:

$$\rho C_V \frac{\partial T}{\partial t} = k_T \frac{1}{r^{\alpha-1}} \frac{\partial}{\partial r}\left(r^{\alpha-1}\frac{\partial T}{\partial r}\right) + Q_S. \quad (6)$$

Here T is the temperature, k_T is the coefficient of thermal conductivity of the medium, the value of Q_S in the equation (6) is determined by the energy release source: $Q_S = I(r,t)\, k_{abs}$, where k_{abs} is the absorption coefficient of the absorbing particle; $I(r,t) = I_0 f_t(t)\, f_r(r)$ is the intensity of the light beam. A power-exponential function $f_t(t) = \frac{t}{\tau_\text{p}} e^{-\frac{t}{\tau_\text{p}}}$ has been chosen as a temporal shape of the laser pulse, where τ_p is the duration of the laser pulse. The spatial function has the form $f(r) = 1$, when $r \le R_0$, and $f(r) = 0$, when $r > R_0$.

The solution of the system of equations (1)–(6) makes it possible to calculate the space-time dependencies of pressure, temperature, density, and velocity, to estimate contribution of thermal and acoustic mechanisms to the change in the physical parameters of a continuous medium.

Numerical modeling of the system of equations of motion in the Lagrange form has been carried out using the method of finite-difference approximation described in [10] taking into account the introduction of pseudoviscosity, which makes it possible to stabilize the numerical solution in the region of the existence of pressure surges; heat conduction equation have been solved according to the three-layer explicit scheme presented in [12].

When implementing the numerical method, the computational domain has been divided into cells of size $\Delta r = 10^{-3} R_0$ (R_0 is energy release area size) with the maximum number of cells 10000. The time step was determined by the well-known Courant criterion $\Delta t = k\frac{\Delta r}{u_0}$, where the coefficient $k = 0.01 \div 0.1$.

For cylindrical and spherical geometry of the problem ($\alpha = 2, 3$) the boundary condition of the form $u(r=0) = 0$ has been used, which reflects the zero velocity at the point $r = 0$ at any time moment. In plane geometry ($\alpha = 1$) the free boundary of the medium is assumed $P(r=0) = 0$.

3. Numerical results and discussion

In the problem with flat geometry ($\alpha = 1$), we assume that pulsed laser radiation from a wide light beam is absorbed by a thin film of material (a thin layer of graphite) located on the surface of a liquid (water). Let us discuss the material parameters for this task. The in-plane thermal conductivity of a bulk graphite at room temperature is about $k_T = 2$ W/cm K [13], but the theoretical evaluation for nano- and microparticles, where phonons are confined, shows much lower values such as $k_T = 0.7$ W/cm K [14]. But for out-of-plane thermal conductivity considered in the article the theoretical and experimental results are quite consistent and give the value of $k_T = 0.06$ W/cm K [13–15]. The specific heat capacity is similar for bulk and micro-sized graphite and is taken as $C_V = 0.7$ J/g K [16, 17]. Other parameters of graphite used in computations are the following: density $\rho_0 = 2.3$ g/cm^3 [13], absorption coefficient in the neat IR region $k_{abs} = 4 \cdot 10^4$cm^{-1} [18], speed of sound $u_0 = 2.2 \cdot 10^6$cm/s [19], and Grüneisen coefficient $\Gamma = 2$ [20]. For water, the absorption coefficient was assumed to be equal to zero, and typical thermophysical parameters were used (density $\rho_w = 1$ g/cm^3, sound speed $u_w = 1.5 \cdot 10^5$cm/s, thermal conductivity coefficient $k_w = 0.6 \cdot 10^{-3}$W/cm K, volume expansion coefficient $\beta_w = 0.2 \cdot 10^{-3}$K^{-1}). It was assumed in the calculations that the duration of the laser pulse varies from 100 fs to 10 ps, that are typical for laser systems operating in the mode of generation of ultrashort laser pulses. The intensity varied within $I_0 = 10^4 - 10^6$ W/cm^2, which corresponds to a radiation flux density of the order of mJ/cm^2.

The results of calculating the change in temperature ΔT, pressure ΔP, speed of movement u are shown in Fig. 2. As it can be seen, when the energy of a short laser pulse (0.5 ps) is absorbed in a thin (110 nm) graphite layer, it is locally heated (Fig. 2), and the pressure increases (Fig. 2b). The presence of a pressure gradient

between the region in which the energy release occurred and the undisturbed region inside the medium causes the particles of the medium to move with a positive velocity ($u > 0$) directed deep into the medium (Fig. 2c). At the same time, in the near-surface layer, particles of the medium acquire a negative velocity ($u < 0$) directed to the free space above the surface (Fig. 2c, curves 1-2). Waves of pressure (Fig. 2,b), velocity (Fig. 2,c) and density of the substance, when propagating deep into the medium at the speed of sound in water, are characterized by the presence of positive (volumetric compression) and negative (volumetric rarefaction) phases, as well as retain their positive and negative amplitudes, that is, they are solitary plane waves.

In problems of cylindrical ($\alpha = 2$) or spherical ($\alpha = 3$) geometry, we assume that the release of laser pulse energy occurs in a particle of the corresponding geometry in terms of its optical and thermophysical characteristics similar to a graphite structure.

The results of calculating the changes in pressure $\Delta P(r,t)$, temperature $\Delta T(r,t)$, and velocity $u(r,t)$ of the medium for the case of cylindrical symmetry are shown in Fig. 3, and for spherical geometry - in Fig. 4. After the end of the action of a short laser pulse due to local heating (Figs. 3a, 4a, curve 2) and the presence of a pressure gradient $\Delta P/\Delta r$ (Figs. 3b, 4b, curve 1) between the region in which the energy release occurred, and the unperturbed region, the particles of the environment are involved in motion with a positive velocity ($u(r > R_0),t) > 0$) directed from the center of symmetry (Figs. 3c, 4c, curves 1-5), and form a compression wave front ($\Delta P > 0$, Fig. 3b, 4b, curves 1-5). Due to the presence of the symmetry center of the problem ($r = 0$), when this point is reached, the particle velocity near the center of the energy release region is mirrored to negative ($u(r < R_0),t) < 0$), forming a negative component of the pressure wave $\Delta P < 0$. Thus, the pressure wave (Fig. 3b, 4b) during its propagation in the external medium is characterized by the presence of positive (volumetric compression, $\Delta P > 0$),

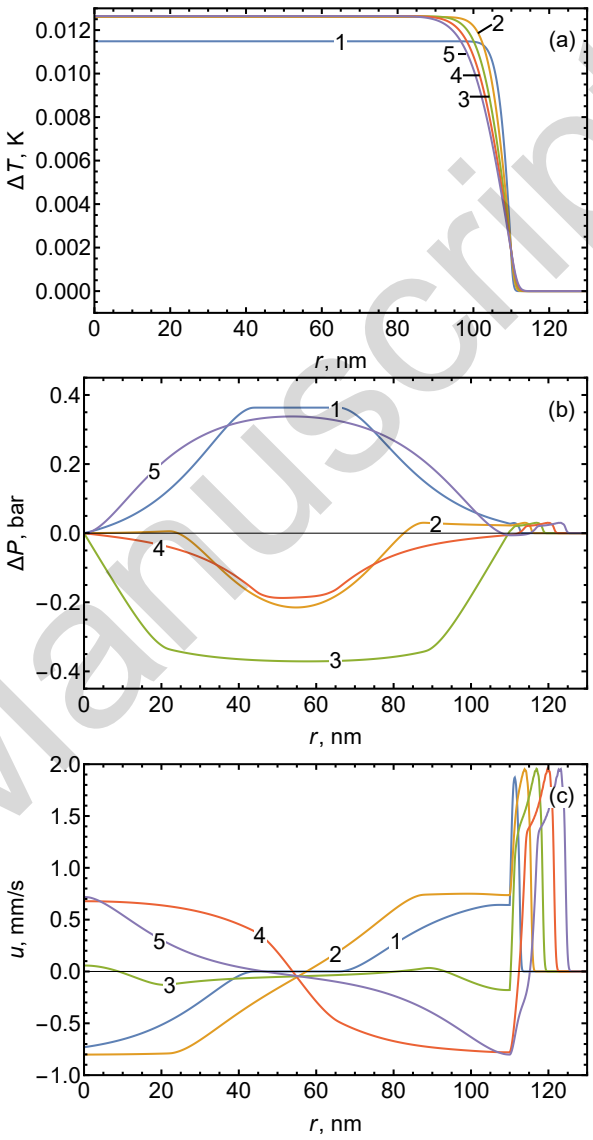

FIG. 2. (color online) Temporal evolution of spatial distribution of temperature increase (a), pressure change (b), and speed (c) for graphite plane layer ($\alpha = 1$, $I_0 = 10^6$ W/cm^2, $t_p = 0.5$ ps, $R_0 = 110$ nm): 1) $t = 2$ ps, 2) $t = 4$ ps, 3) $t = 6$ ps, 2) $t = 8$ ps, 2) $t = 10$ ps.

and negative (volumetric tension, $\Delta P < 0$) phases. Moreover, the minimum values of pressure (in the negative phase) are achieved at the center of symmetry of the problem ($r = 0$).

Next, we consider the long-term dynamics of processes inside and outside graphite nanoparticles. As an example, let us choose

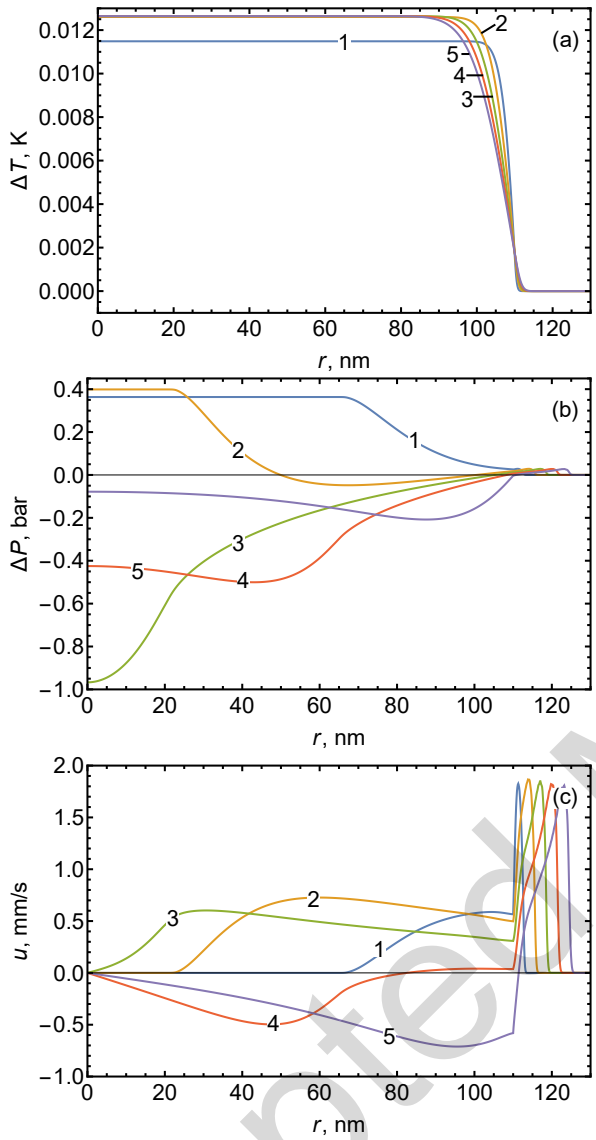

FIG. 3. (color online) Temporal evolution of spatial distribution of temperature increase (a), pressure change (b), and speed (c) for graphite cylindrical particle ($\alpha = 2$, $I_0 = 10^6$ W/cm^2, $t_p = 0.5$ ps, $R_0 = 110$ nm): 1) $t = 2$ ps, 2) $t = 4$ ps, 3) $t = 6$ ps, 2) $t = 8$ ps, 2) $t = 10$ ps.

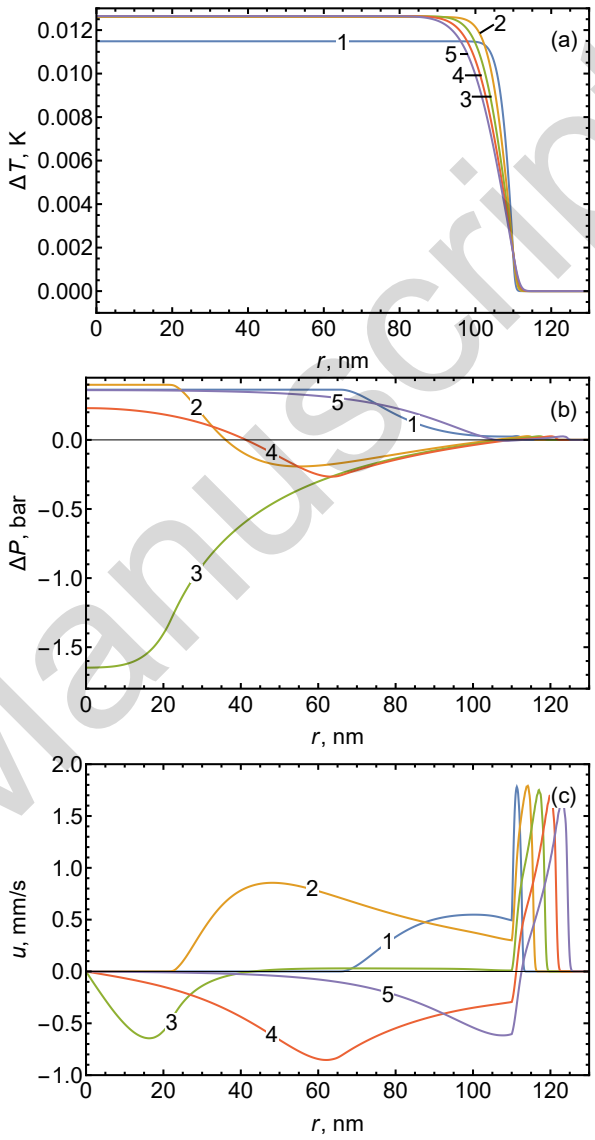

FIG. 4. (color online) Temporal evolution of spatial distribution of temperature increase (a), pressure change (b), and speed (c) for graphite scherical particle ($\alpha = 3$, $I_0 = 10^6$ W/cm^2, $t_p = 0.5$ ps, $R_0 = 110$ nm): 1) $t = 2$ ps, 2) $t = 4$ ps, 3) $t = 6$ ps, 2) $t = 8$ ps, 2) $t = 10$ ps.

a particle of spherical geometry (with a radius of 110 nm). Such a particle can be considered as a spherical resonator for acoustic waves. In this case, the center of symmetry ($r = 0$) is a perfect reflective mirror, and the graphite-water interface is a semitransparent mirror. In this situation, the spatiotemporal evolution of the pressure wave can be considered from the point of view of the evolution of the breathing mode of a given resonator. The time dependencies of the pressure at various points of this resonator and in the environment are shown in Fig. 5.

As it can be seen, the amplitude of the excited acoustic oscillations in the center of the

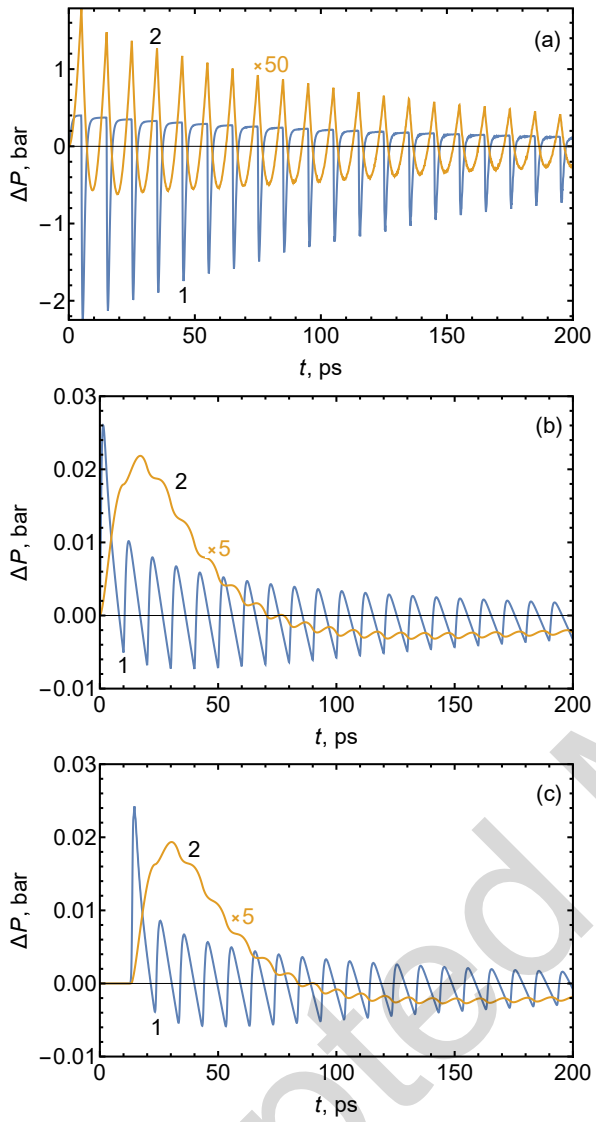

FIG. 5. (color online) Pressure oscillations in the center of graphite particle ($r = 0$ nm) (a), at the particle/water interface ($r = 110$ nm) (b), and in the water ($r = 130$ nm) (c) ($\alpha = 3$, $R_0 = 110$ nm): 1) $I_0 = 10^6$ W/cm^2, $t_p = 0.5$ ps, 2) $I_0 = 5 \cdot 10^4$ W/cm^2, $t_p = 10$ ps.

particle, at the graphite–water interface, and in the surrounding water space significantly depends on the duration of the exciting laser pulse at the same radiation flux density. This effect is related to the efficiency of excitation of acoustic pulses depending on the ratio between the duration of the laser pulse and the time of passage of the acoustic pulse through the absorbing structure. When the condition $\tau_i < t_a = 2R_0/u_0$ is met, one can expect the implementation of the mode of effective excitation of an acoustic pulse in the "short impact" mode, which is subject to the results of numerical simulation presented in Fig. 5.

Also, this mode of excitation of high-frequency vibrations can be associated with the excitation of the radial mode of vibrations of a spherical nanoparticle. Thus, Figure 6 shows a graph of the time dependence of the change in the radius of a spherical graphite nanoparticle after absorption of the energy of a short laser pulse. As can be seen from Fig. 6, the period of radial oscillations is unambiguously related to the particle radius and the acoustic wave propagation time inside the nanoparticle ($t_a = 2R_0/u_0$).

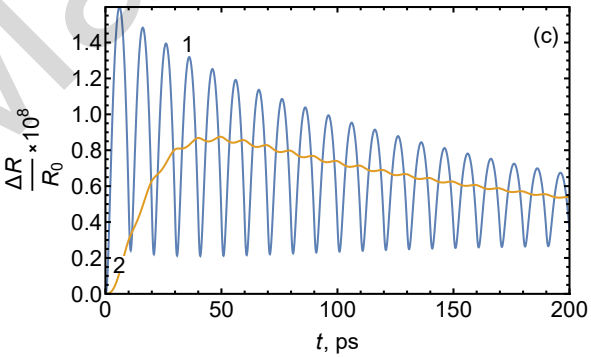

FIG. 6. (color online) Graphite particle oscillations ($\alpha = 3$, $R_0 = 110$ nm): 1) $I_0 = 10^6$ W/cm^2, $t_p = 0.5$ ps, 2) $I_0 = 5 \cdot 10^4$ W/cm^2, $t_p = 10$ ps.

Finally, Fig. 7 shows the generalized dependencies of the pressure amplitude ΔP on the laser pulse duration for various radii of spherical graphite particles and a constant volume density of the energy release. Depending on the ratio between the pulse duration τ_i and the time of passage of a sound wave along the radius of a spherical particle t_a, various options for excitation of acoustic oscillations are realized. In the case of short laser pulses ($\tau_i < t_a$), the amplitude of the bipolar pressure wave reaches maximum values both in the positive (Fig. 7a) and negative (Fig. 7b) phases. At the same time, in the limit

of long-term laser pulses, the acoustic response of the medium to the acting pulsed radiation is negligibly small.

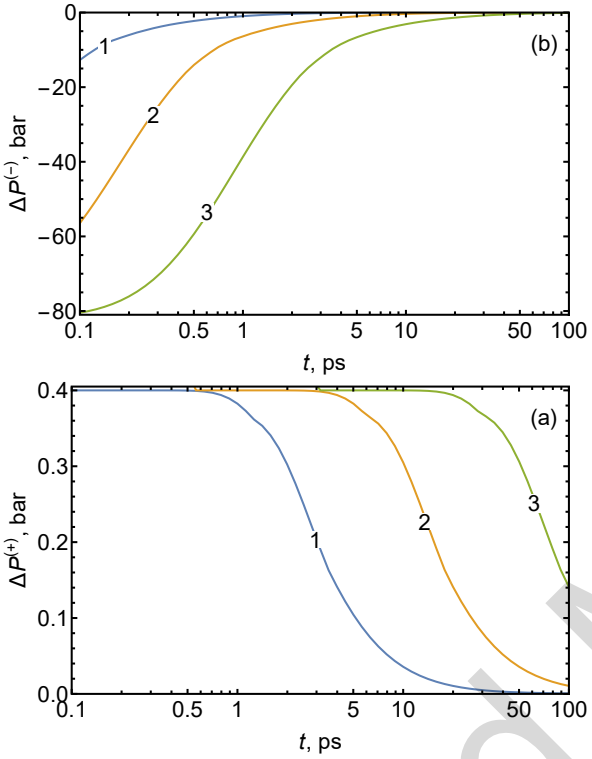

FIG. 7. (color online) Maximum (a) and minimum (b) pressure difference vs. laser-pulse duration for different spherical ($\alpha = 3$) particle sizes: 1) 110 nm, 2) 550 nm, 3) 2.75 μm. The fluence $\Phi = t_p I_0 = 0.5\ \mu\text{J/cm}^2$ remains the same for all points.

4. Conclusions

To summarize we note that the developed technique for modeling the optoacoustic response of carbon-containing nano- and microstructures in an aqueous environment, based on solving the equations of motion of continuous media in the Lagrange form, has demonstrated the ability to calculate main thermodynamic characteristics of media and predict the effects of high-amplitude exposure to pulsed laser radiation, for example, on biological objects. Spatio-temporal dependencies of pressure waves, medium particle velocity, and material density have been calculated for various laser pulse durations and sizes of nano- and microparticles in three geometries: flat, cylindrical, and spherical. During the computational experiment, the optimal values of laser pulse durations for excitation of acoustic signals in these structures were established. The results of modeling in spherical geometry allow us to explain the experimental results on the destruction of cancer cells under the influence of picosecond pulsed radiation [21]. Further development of the studies on interaction of short laser pulses with carbon nano- and microstructures will make it possible to find new promising theranostic agents.

Acknowledgments

This research was supported within the framework of the State Program for Fundamental Research "Photonics and Electronics for Innovations" (Republic of Belarus), project 1.17.1 "Modeling and creation of photonic and optoelectronic nanostructures based on graphene-like materials for controlling optical radiation".

References

[1] A. Attia, G. Balasundaram, M. Moothanchery, U. Dinish, R. Bi, V. Ntziachristos, and M. Olivo, A review of clinical photoacoustic imaging: Current and future trends. Photoacoustics **16**, 100144 (2019).

[2] D. Dumitras, M. Petrus, A. Bratu, and C. Popa,

Applications of Near Infrared Photoacoustic Spectroscopy for Analysis of Human Respiration: A Review. Molecules **25**, 1728 (2020).

[3] P. van Capel, E. Peronne, and J. Dijkhuis, Nonlinear ultrafast acoustics at the nano scale. Ultrasonics **56**, 36 (2015).

[4] R. Smith, F. P. Cota, L. Marques, X. Chen, A. Arca, K. Webb, J. Aylott, M. Somekh, and M. Clark, Optically excited nanoscale ultrasonic transducers. J. Acoust. Soc. Am. **137**, 219 (2015).

[5] A. Taruttis and V. Ntziachristos, Advances in real-time multispectral optoacoustic imaging and its applications. Nature Photonics **9**, 219 (2015).

[6] O. Romanov, G. Zheltov, and G. Romanov, Thermomechanical effect of ultrashort laser pulses on single-dimension metallic nanostructures. Bulletin of the Russian Academy of Sciences: Physics **78**, 1299 (2014).

[7] N. Khokhlov, G. Knyazev, B. Glavin, Y. Shtykov, O. Romanov, and V. Belotelov, Interaction of surface plasmon polaritons and acoustic waves inside an acoustic cavity. Optics Letters **42**, 3558 (2017).

[8] O. Romanov, G. Zheltov, and G. Romanov, Numerical modeling of thermomechanical processes in absorption of laser radiation in spatially inhomogeneous media. Journal of Engineering Physics and Thermophysics **84**, 772 (2011).

[9] Y. Zel'dovich and Y. Raizer, *Physics of Shock Waves and High Temperature Hydrodynamic Phenomena (in Russian)* (Moscow: Nauka, 1966).

[10] R. Richtmayer and K. Morton, *Difference methods for initial-value problems* (New-York. John Wiley and Sons, 1967).

[11] D. Kanel', S.V.Razorenov, A. Utkin, and V. Fortov, *Shock–Wave Phenomena in Condensed Media (in Russian)* (Moscow: Yanus–K, 1996).

[12] F. Fanjul-Velez, J. Arce-Diego, and O. Romanov, Efficient 3D numerical approach for temperature prediction in laser irradiated biological tissue. Computers in Biology and Medicine **39**, 810 (2009).

[13] C. Ho, R. Powell, and P. Liley, Thermal Conductivity of the Elements. Journal of Physical and Chemical Reference Data **1**, 279 (1972).

[14] L. Paulatto, F. Mauri, and M. Lazzeri, Anharmonic properties from a generalized third-order ab initio approach: Theory and applications to graphite and graphene. Phys. Rev. B **87**, 214303 (2013).

[15] A. Balandin, Thermal properties of graphene and nanostructured carbon materials. Nature Mater **10**, 569 (2011).

[16] N. Pradhan, H. Duan, J. Liang, and G. Iannacchione, The specific heat and effective thermal conductivity of composites containing single-wall and multi-wall carbon nanotubes. Nanotechnology **20**, 245705 (2009).

[17] S. Picard, D. Burns, and P. Roger, Determination of the specific heat capacity of a graphite sample using absolute and differential methods. Metrologia **44**, 294 (2007).

[18] T. Smausz, B. Kondász, T. Gera, T. Ajtai, N. Utry, M. Pintér, G. Kiss-Albert, J. Budai, Z. Bozóki, G. Szabó, and B. Hopp, Determination of UV–visible–NIR absorption coefficient of graphite bulk using direct and indirect methods. Applied Physics A **123**, 633 (2017).

[19] X. Cong, Q.-Q. Li, X. Zhang, M.-L. Lin, J.-B. Wu, X.-L. Liu, P. Venezuela, and P.-H. Tan, Probing the acoustic phonon dispersion and sound velocity of graphene by Raman spectroscopy. Carbon **149**, 19 (2019).

[20] P. Klemens and D. Pedraza, Thermal conductivity of graphite in the basal plane. Carbon **32**, 735 (1994).

[21] L. Golubewa, I. Timoshchenko, O. Romanov, R. Karpicz, T. Kulahava, D. Rutkauskas, M. Shuba, A. Dementjev, Y. Svirko, and P. Kuzhir, Single-walled carbon nanotubes as a photo-thermo-acoustic cancer theranostic agent: theory and proof of the concept experiment. Scientific Reports **10**, 22174 (2020).